Journal of Medicinal Chemistry

Article

pubs.acs.org/jmc

A Low Cytotoxic Cationic Metal–Organic Framework Carrier for Controllable Drug Release

Quan Hu,[†] Jiancan Yu,[‡] Min Liu,[‡] Aiping Liu,[‡] Zhongshang Dou,[‡] and Yu Yang*[,‡]

[†]Department of Pharmacology, School of Medicine, Hangzhou Normal University, Hangzhou 310036, PR China

[‡]State Key Laboratory of Silicon Materials, Cyrus Tang Center for Sensor Materials and Applications, Department of Materials Science & Engineering, Zhejiang University, 38 Zheda Road, Hangzhou 310027, PR China

Supporting Information

ABSTRACT: A positively charged porous drug carrier MOF-74-Fe(III) (**1**, MOF = metal–organic framework), which could not be directly synthesized using ferric salts, was prepared through the oxidation of the neutral crystal MOF-74-Fe(II). This cationic host material exhibits very low cytotoxicity upon PC12 cells by 3-(4,5-dimethylthiazol-2-yl)-2,5-diphenyl tetrazolium (MTT) assay and high drug loading capacity of ibuprofen anions (~15.9 wt %) through ion exchange and salt penetration procedures. Controlled by anion exchange, two mechanisms were involved in the drug release process with different drug delivery rates due to the presence of coordinated or free ibuprofen anions, making the administration of drug release more flexible.

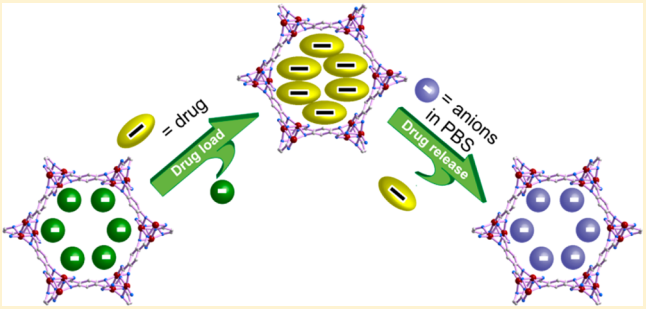

INTRODUCTION

Porous metal–organic frameworks (MOFs) have attracted considerable interests for the applications in gas storage and separation,[1] catalysis,[2] and recently as promising platforms for functional molecular materials[3] such as luminescent sensors[4] and drug delivery.[5] The intrinsic nature of MOFs generally endows them with excellent biodegradability, biocompatibility, and guests loading capability, providing promising candidates as drug delivery hosts.[5] In particular, the facile integration of multifunctional components via inclusion and surface chemistry in individual MOF crystals, together with the mature synthesis method in nanoscale, has facilitated multitarget medicine applications in both diagnosis and therapy. In this concern, tremendous efforts on MOF carriers have been made to pave their way toward medical applications.[6]

In drug delivery systems, the administration of drug release profiles, typically to prevent the burst release effect or to keep the drug concentration at a certain required level for a long period, is important to improve product efficacy and safety. This process is mainly related to the carrier–drug interaction. In the MOF/drug systems, interactions which govern the diffusion and release of drugs could be ascribed to van der Waals' force, hydrogen bonds, coordination bonds, $\pi-\pi$ interaction, and anions–cations electrostatic interaction between drugs and frameworks. Among them, the strong electrostatic interaction between ionic drugs and ionic frameworks has attracted particular interests because the release of ionic drug is a chemical stimuli-responsive process taking place only through ion exchange. For instance, Rosi and Su et al. have successfully adopted anionic MOFs as cationic drug to control the drug release programming.[7]

Recently, Fe-based MOFs are presented as a category of biomedical materials with low toxicity, which have been widely used by Horcajada and Lin et al. as delivery host materials.[5,8] More interestingly, the possible oxidation of Fe(II) nodes toward Fe(III) will render neutral frameworks bearing additional positive charges, which allow the selective encapsulation of anionic drug, e.g., carboxylate and sulfonate derivatives. Herein, we demonstrated an approach to developing a Fe(III)-based cationic framework that could not obtained directly from the reaction of Fe(III) salts with linkers. MOF-74, which has different variants containing various metal nodes such as Zn^{2+},[9] Mg^{2+},[10] Co^{2+},[11] Ni^{2+},[11] and Fe^{2+},[12] represents a class of porous materials with intriguing performance, and recently MOF-74-Mg has been theoretically predicted as a potential drug carrier.[13] Using a neutral MOF-74-Fe(II) ($Fe(II)_2$(dobdc), $dobdc^{4-}$ = 2,5-dioxido-1,4-benzenedicarboxylate) as starting materials, positively charged framework counterparts, MOF-74-Fe(III) (**1**), were prepared through a postoxidation procedure (see Figure 1). The cytotoxicity, drug uptake, and release behavior of microcrystal **1** was evaluated and discussed.

RESULTS AND DISCUSSION

The solvothermal reaction of ferrous salts $FeCl_2$ with H_4dobdc afforded dark-red microcrystals MOF-74-Fe(II) (CPO-27-

Received: March 15, 2014
Published: June 12, 2014

   dx.doi.org/10.1021/jm5004107 | J. Med. Chem. 2014, 57, 5679–5685

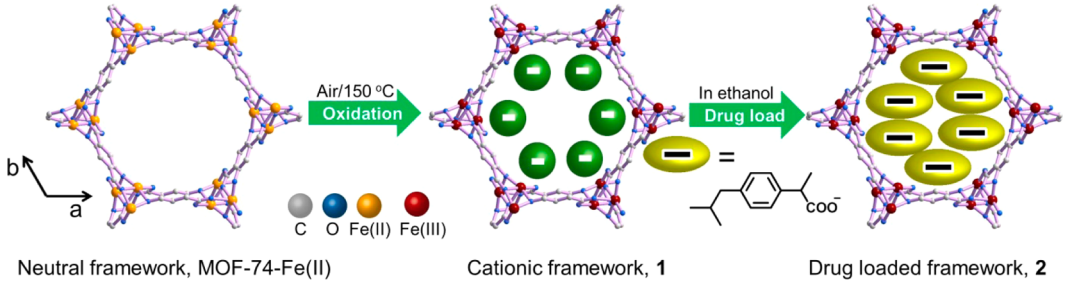

Figure 1. Schematic presentation of the process of MOF-74-Fe(II) oxidation to crystal **1** and drug loading.

Fe(II)), which are readily suffered from oxidation in the air, as reported by Long et al.[12] To introduce additional positive charges of the network, the oxidation reaction of the Fe(II) nodes was conducted in the air at 150 °C for 20 min, resulting in black powders. The oxidation of the porous solid was identified by X-ray photoelectron spectroscopy (XPS). As shown in Figure 2, the Fe $2p_{3/2}$ XPS peak of the sample treated

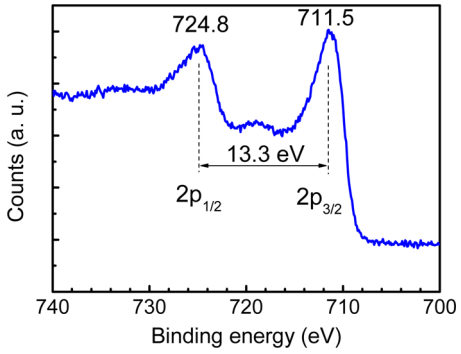

Figure 2. Fe 2p XP spectra of the samples after heated at 150 °C in the air.

in the air was found around 711.5 eV, similar to that of Fe_2O_3,[14] suggesting the sample is oxidized to ferric compound thoroughly, largely owning to the porous nature of MOF-74-Fe(II), where Fe^{2+} cations are exposed to the inside of crystal channels. The powder XRD pattern of simulated crystal **1** and a synthesized one are shown in Figure 3, and the matching curves indicate the formation of the MOF-74-Fe(III) phase. SEM image of the sample in Figure 4a reveals that the morphology of the porous crystals is hexagonal rods with a width ranging from 200 to 800 nm.

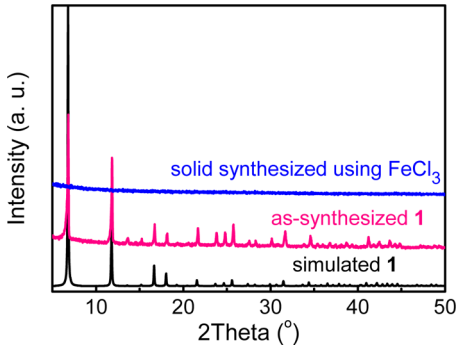

Figure 3. PXRD patterns of simulated (black),[12] as-synthesized (pink) crystal **1**, and solid synthesized using H_4dobdc and $FeCl_3$ (blue).

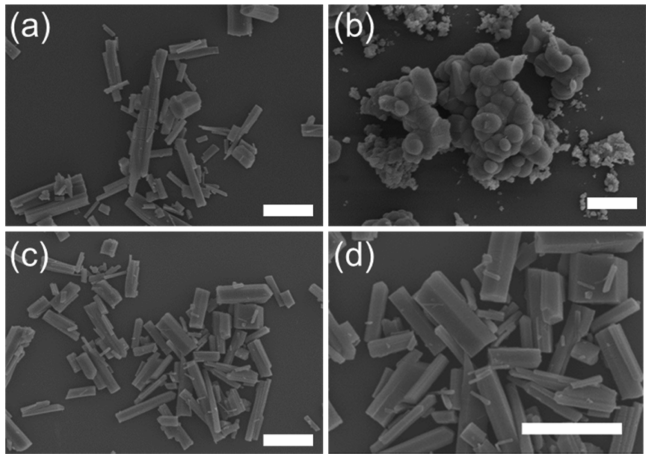

Figure 4. SEM images of materials. Microcrystals **1** oxidized from MOF-74-Fe(II) (a), amorphous solid synthesized from $FeCl_3$ and H_4dobdc under the same procedure (b), and drug loaded crystals **2** (c,d). Scale bar, 2 μm.

As suggested by Bloch et al., the ferrous MOF-74-Fe(II) exhibits reversible adsorption of O_2 at a relatively low temperature (252 K), generating ferric crystal **1** with the superoxide anions (O_2^-) as counterions, which are likely to undergo the dismutation reaction and yield hydroxide in the presence of water in the air. The binding of hydroxide anions through the dismutation reaction makes the oxidative product irreversible. In addition, the oxidation of the neutral ferrous MOFs consequently results in additional two positive charges for a moiety of Fe_2(dobdc), forming a ferric MOFs $[Fe_2(dobdc)]^{2+}$, which are balanced by hydroxide anions OH^-. The cation density in the resulting solid reaches a very high value of 7.6 mmol/cm^3, about 9-fold of that for an anionic bio-MOF-1 served as drug carriers.[7a] We also tried to synthesize cationic porous materials by using ferric salt $FeCl_3$ directly instead of $FeCl_2$, only yielding amorphous products (Figures 3 and 4b). The failure of direct synthesis of cationic MOFs suggests that Fe^{2+} plays a crucial role in the formation of the secondary building units (SBUs) of the crystals, and the postoxidation strategy provides a facile approach to obtaining charged porous materials or carriers with required structure and morphology.

As shown in Figure 1, MOF-74 series crystals have hexagonal 1D channels in a diameter of around 1.10 nm along the *c*-axis for dehydrated samples.[9] This large accessible opening allows accommodating of guest molecules in large sizes such as drugs and dyes. As a model drug for analgesic and anti-inflammatory treatment, ibuprofen has been extensively used to study the controllable delivery and release capability of drug carriers.[8c,15] The ibuprofen molecule contains a carboxyl group, which can

dx.doi.org/10.1021/jm5004107 | J. Med. Chem. 2014, 57, 5679−5685

be deprotonated by NaOH solution, forming ibuprofen anion Ibu^-. The penetration of sodium ibuprofen and ion exchange of hydroxide anions resided in the cationic porous solid with the drug anions was accomplished in the ethanol solution. The resulting solid was analyzed with IR spectra, in comparison with the host materials. After immersing in the NaIbu solution for 6 d, an additional absorption band around 2890 cm^{-1} is observed with respect to the pristine crystal **1**, which is ascribed to the vibration of C−H in alkyl moiety of ibuprofen (see Figure 5),

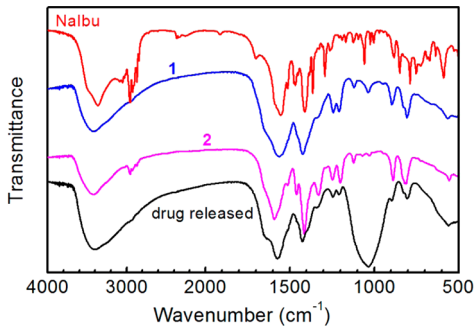

Figure 5. IR spectra of deprotonated ibuprofen by NaOH, NaIbu (red), oxidized crystal **1** (blue), drug loaded composite **2** (pink), and drug released solid in the PBS solution for 12 h (black).

indicating the encapsulation of ibuprofen. The content of drug included in the porous materials was evaluated by elemental analysis (See Experimental Section). Atomic absorption spectra reveal the existence of sodium cations, with a Na/Fe mass ratio of about 1/59. In combination of elemental analysis results, ~13.5 mol % of hydroxide anions were exchanged with drug anions, and ~23% Ibu^- exists as the sodium salt. The drug load capacity is around 0.21 g for 1 g of dried materials, corresponding to 15.5 wt % in the resulting composite **2**. The morphology of the yielding was also studied by SEM. As shown in Figure 4c,d, the encapsulation of ibuprofen does not change the morphology and no significant layers are observed on the surface of microcrystals, indicating drug molecules are well dispersed in the channels of the porous materials, which is required by drug delivery systems. Furthermore, the crystalline feature of **2** retains the phase of **1**, as identified by powder XRD (Supporting Information Figure S1), and they are stable in the dry air even for 1 month. It should be noted that the presence of Ibu^- anions in the channels of MOFs would be ascribed to two different categories. As crystal **1** contains a large amount of unsaturated metal sites after removal of coordinated water and hydroxide anions, the deprotonated carboxyl groups are likely to coordinate with Fe atoms. Other Ibu^- anions, including in the form of sodium salt, would be distributed as free anion randomly in the channels. Thus, dramatic variation in the drug release kinetics would be predicted.

We choose PC12 cells as the model to evaluate the cytotoxicity by MTT assay and by microscopy because they are vulnerable to oxidative stress,[16] which is likely to be provided by this ferric compound **1**. The adhesion nature of this kind of cells to culture plate makes MTT assay possible, and therefore PC12 cell line is a widely used cellular model to evaluate the cytotoxicity of nanomaterials.[17] Furthermore, PC12 cells are neuron cells with enriched neurites, whose morphology reflects their state and could be easily visualized by microscopy. The MTT assay determines the ability of a viable cell's mitochondria to reduce the MTT into formazan.[18] The decline of MTT to formazan indicates the decrease in mitochondrial metabolism of the cells. Therefore, the absorbance of formazan directly correlates to the number of cells. It is suggested that the introduction of low-concentration MOFs can barely change the cytotoxicity profile of MOFs on PC12 cells (Figure 6). The viability of cells maintains at about

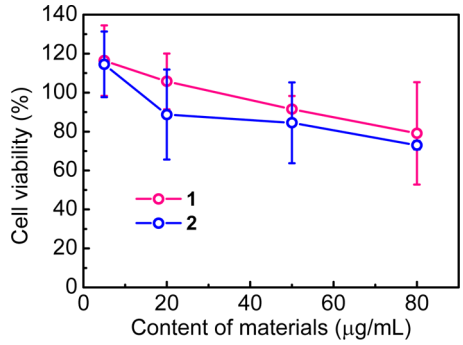

Figure 6. Cell viability data of MOFs obtained from cultured PC12 cells with the untreated cell as a control. Error bars represent the standard deviation of uncertainty for each point.

100% after incubating with two MOFs probes at 5 μg/mL for imaging experiments (Figure 7). The cells attach, survive, and

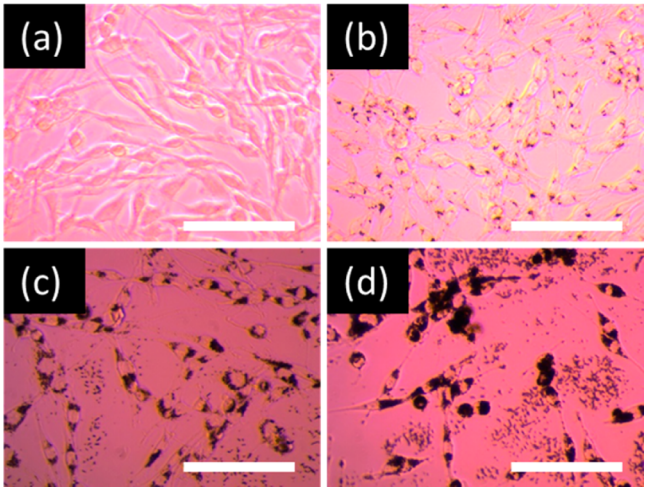

Figure 7. Optical microscopy images of living PC12 cells after 12 h exposure to crystal **1**at (a) 0 μg/mL, (b) 5 μg/mL, (c) 20 μg/mL, and (d) 50 μg/mL. Scale bar, 50 μm.

emit long neuritic processes (neurites). No significant difference neither in the density nor morphology of the cell can be detected between cells incubated with MOFs and the control ones (Figures 7a,b and 8a,b). In comparison with composite **2**, **1** crystals are accumulated in the intracellular space around the nuclei, which is probably caused by the electrostatic interaction between cationic frameworks and negatively charged surface of PC-12 cells (Figures 7 and 8). The dose response of MOFs on PC12 cells shows the decrease in the reduction of MTT to formazan with the increasing MOF concentration. In the case of 50 μg/mL crystal **1**, although the density of cell number decreases with respective to samples of lower MOFs concentration, both the close adhesion of incubated cells to the substrate and the desirable appearance of neurites emitting indicate the low toxicity of crystal **1** even at a high concentration (Figure 7d).

dx.doi.org/10.1021/jm5004107 | J. Med. Chem. 2014, 57, 5679−5685

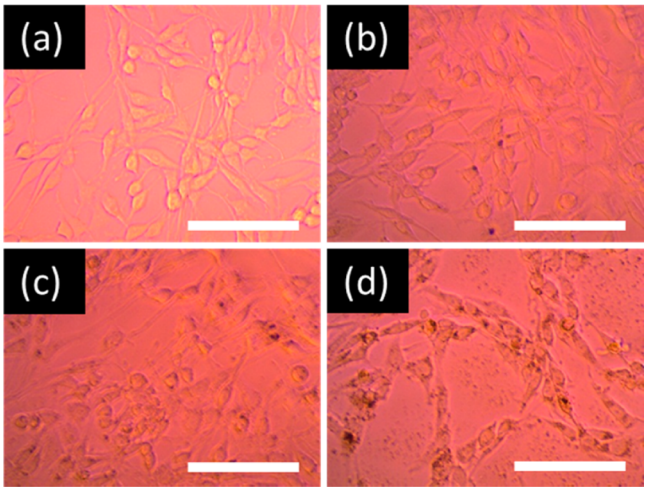

Figure 8. Optical microscopy images of living PC12 cells after 12 h exposure to **2** at (a) 0 μg/mL, (b) 5 μg/mL, (c) 20 μg/mL, and (d) 50 μg/mL. Scale bar, 50 μm.

The bright-field and confocal microscopy images of fixed PC12 cells incubated with 5 μg/mL crystal **1** are shown in Figure 9. The morphology, size, and appreciable neurite

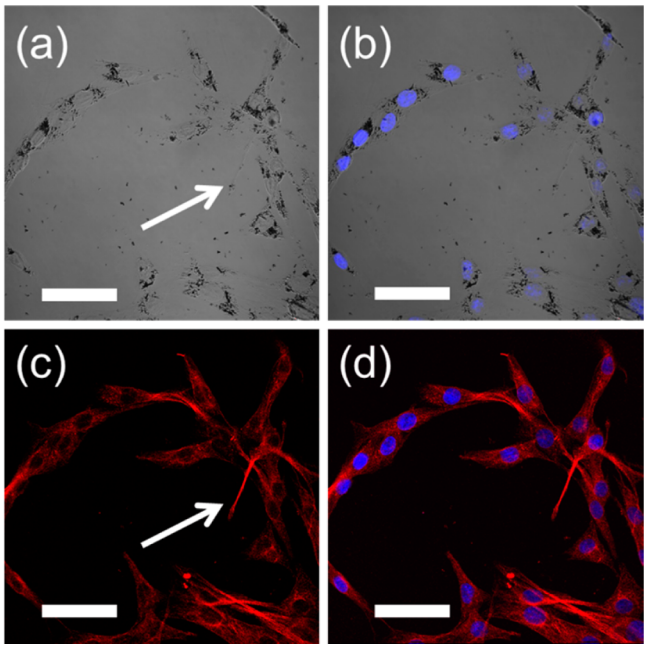

Figure 9. Bright-field (a), fluorescence (b,c), and overlapped (d) confocal microscopy images of fixed PC12 cells incubated with 5 μg/mL **1** for 12 h and the intracellular distribution of **1**. Microtubular cytoskeleton (tubulin, red) and nuclei (blue) were fluorescently stained. Scale bar, 50 μm.

extension of cells are maintained after incubation. Many MOFs clusters are observed and segregated in the cytosol by the endocytosis. In some cells, MOFs are enriched in the growth cone of neurites. Immunological staining of cell microtubular cytoskeleton (tubulin-red) and nuclei (blue) shows the spreading, expansion, and communication of cells with each other, exhibiting a distinctive outgrowth of axons and dendrites. It is indicated that the crystal **1** is low toxic or nontoxic for neuron survival nor does it impair neurite outgrowth.

Figure 10 shows the release profiles of the drug delivery system of **2** in PBS solution (pH = 7.4) at 37 °C. A steady

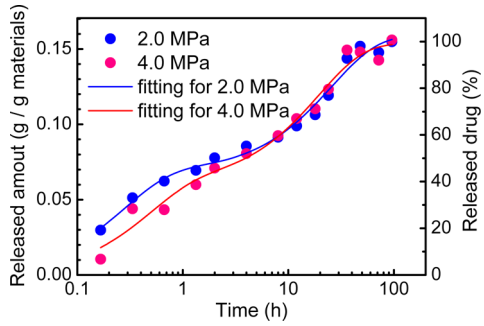

Figure 10. Release profiles of Ibu^- in PBS solution for drug pellets compacted under 2.0 and 4.0 MPa, respectively.

release of ibuprofen anions was observed in all phases before the depletion of drugs, with a fast release during the first several hours, and then followed by a slower counterpart. It is estimated that half amount of drug was released in 4 h, and the other part released gradually, implying a couple of possible release mechanisms involved in this process. As discussed previously, there are two distinctive presence environments of Ibu^- anions in host channels, resulting in the dramatically different release behaviors between two types of anions. Thus, a first-order release kinetic models[19] is applied with two-component formula to fit the release amount after immersing the drug@MOF solid into the PBS solution for a period of t h

$$m = m_0(1 - A_1e^{-a_1t} - A_2e^{-a_2t})$$

where m_0 and m are the initial and released Ibu^- mass for 1 g drug delivery, respectively, and A_1, A_2, a_1, and a_2 are the weight and kinetic fitting parameter for the drug release involving two mechanisms with $A_1 + A_2 = 1$. The well fitted results (R^2 = 0.9887, 0.9881 for pellets prepared under 2.0 and 4.0 MPa pressure, respectively) do indicate the existence of two processes contributed to the drug release. For the pellet compacted under 2.0 MPa, the fitting formula is expressed as

$$m = 0.1589(1 - 0.5711e^{-0.3858t} - 0.4289e^{-3.595t})\text{g}$$

The value of m_0, 0.1589, is consistent with the elemental analysis result which is estimated to be 15.5%. Besides, the fact that the weights A_1 and A_2 are comparable to each other and the parameters relative to the release rates, a_1 and a_2 are different in an order, indicating that both release processes are equally contributed to resulting release rate.

Except the sodium ibuprofen (~23%), the drug release is governed by the interaction between the positive charged host porous materials and negatively charged drug, and the ratio of two kinds of ibuprofen anions can be identified by analyzing the release evolution formula. Initially, the released drug is mainly sodium ibuprofen and the other coordinated free anions, which are governed by the rate of merely diffusion or ion exchange taking place both inside the nanochannels and the interface between drug-encapsulated materials and PBS solution. As the delivery host is in nano- to micrometer scale, high concentrations of anions Cl^- and PO_4^{3-} in PBS solution readily access to the surface of tiny crystals, resulting in the fast anion exchange. This process corresponds to the item

dx.doi.org/10.1021/jm5004107 | J. Med. Chem. 2014, 57, 5679−5685

$0.4289e^{-3.595t}$, indicating the content of NaIbu and free Ibu^- anions weights of 43%. This rapid drug release stage generally rises to burst release effects if it dominates the whole drug release process. However, it is occasionally required, especially in the case that involved with multiple drug release mechanisms of different rate, because many drugs function only when the drug concentration reaches a critical level.

The following release process of coordinated drug is triggered by phosphate anions because of the preferential coordination of PO_4^{3-} anions with iron cation. In the IR spectra of drug released residue (Figure 5), a significant absorption band around 1050 cm^{-1} due to phosphate is observed, suggesting the involvement of phosphate anions in the drug release process. Furthermore, it is suggested by the additional peak observed in the HPLC results when the solids were soaked in PBS solution for more than 10 h that the release of the drug. The possible decomposition of MOF carrier was further clarified by fluorescence assay of the drug released PBS solution (after 7 d), as the released $dobdc^{4-}$ anions emit characteristic yellowish-green fluorescence around 535 nm (see Supporting Information Figure S2). The release of ligand anions (~10.3 wt %) indicates that the drug release process is accompanied by gradual decomposition of porous materials in the later stage, resulting in amorphous powders with the main ingredients of Fe^{3+}, K^+, and PO_4^{3-} ions (Supporting Information Figures S3–S4). It should be mentioned that the degradable activity of drug carrier is generally required in the clinical application.

In all, the different interaction of two kinds of drug anions with the carriers, free and coordinated, leads to two distinctive drug release stages in this drug delivery system. Precise control over the content of the coordinated anions drug will tame the release kinetics, consequently making the drug work as designed. It could be also envisaged that the drug release at the initial stage might be regulated by changing the size of host porous materials or further encapsulating these materials in other matrices, such as phase-change materials (PCMs),[20] to form controllable drug delivery with hierarchical structures.

CONCLUSIONS

In conclusion, we present a novel cationic porous drug carrier MOF-74-Fe(III) via postoxidation procedure. The low cytotoxicity, efficient drug loading capacity (~15.9 wt %), and controllable release make it a promising drug delivery host. The two distinct release kinetic processes due to the interaction difference of drug cations with frameworks reveal that controlling coordinated drug ratio is a facile way to administrate the drug release profiles. Further precise control of drug release in such a delivery system could be accomplished through regulating the carrier size and encapsulating them into other stimuli-responsive matrices.

EXPERIMENTAL SECTION

Chemistry. 1,4-Dihydroxyterephthalic acid (98%, TCI) and other reagents were obtained from commercial resources without further purification. XRD patterns were taken on a PANalytical X'Pert Pro powder X-ray diffractometer. FTIR spectra were performed on a Thermo Fisher Nicolet IS10 infrared spectrometer. XPS of Fe 2p was taken on a Thermo Fisher ESCALAB 250Xi XPS spectrometer. Elemental analysis was taken on ThermoFinnigan Flash EA 1112 elemental analyzer. The morphology of the crystals was visualized using a Hitachi S-4800 field emission scanning electron microscope. Olympus FV-1000 confocal laser scanning microscope and IX-71 inverted microscope were used to analyze the cell proliferation and the distribution of drug carriers.

*MOF-74-Fe(III) (**1**).* Microcrystals of MOF-74-Fe(II) were synthesized according to the literature.[12] To avoid the oxidation of ferrous cations, a Schlenk technique was applied. To a Schlenk bottle, 1,4-dihydroxyterephthalic acid (1.77 mmol, 349.7 mg), *N*,*N*-dimethylformamide (DMF, 150 mL), and EtOH (20 mL) were added. The air in the bottle was evacuated and charged with argon, and this procedure was repeated for 3 times. After that, a solution of iron(II) chloride tetrahydrate (4.72 mmol, 938.0 mg) in H_2O (20 mL) with trace HCl and Fe powder was introduced to the previous solution using a syringe, and the mixture was stirred at 120 °C for 4 h (stirring speed, 400 rpm). After cooling the mixture, the precipitation was filtered and washed with DMF and EtOH to yield dark-red solid MOF-74-Fe(II). The resulting powder was kept at 150 °C in the air for 20 min to afford crystal **1** with a width range 200–800 nm and length of several micrometers.

*Ibu@MOF-74-Fe(III) (**2**).* Microcrystals **1** (500 mg) in sodium ibuprofen (0.4 M, 10 mL, in ethanol) solution were stirred at 60 °C for 6 d. The resultant solid was filtered, washed with EtOH, and dried in vacuo to yield ibuprofen-containing solid. Elemental analysis for $Fe_2(C_8H_2O_6)(C_{13}H_{17}O_2)_{0.27}(OH)_{1.73}\cdot 3H_2O\cdot 0.08NaC_{13}H_{17}O_2$ (462.94), Calcd C, 32.56; H, 3.41; N, 0. Found: C, 32.46; H, 3.13; N, 0.18. AAS, Na/Fe = 1/59.

Cell Culture, Imaging, and MOFs Cytotoxicity. Rat pheochromocytoma (PC12) cells were incubated in Dulbecco's Modified Eagle's Medium (DMEM, Neuronbc) with 10% fetal bovine serum (FBS) and 1% penicillin/streptomycin (P/S, Boster) for 2–3 days in a humidified incubator (37 °C, 5% CO_2). The cytotoxicities of crystal **1** and **2** were evaluated by using standard MTT assay in a 96-well plate to assess the viability of cultured cells. After 24 h cell incubation in the humidified incubator, two MOFs with different concentrations (5, 20, 50, and 80 μg/mL) were added to the wells and incubated with the PC 12 cells for another 4 h in the incubator. After that, 1× MTT solutions were added to each tested wells and incubated for 4 h. All media were removed, and 150 μL of dimethyl sulfoxide was added to the wells. The absorbance of each sample at 490 nm was measured using a microplate reader, and the morphologies of all cells were observed using an optical microscopy. The cell viability was calculated as the ratio of the absorbance of the sample well to that of the cell control and expressed as a percentage. All experiments were sextuplicated, and the results were averaged.

For imaging experiments, the cells (10^4 cells/mL) were seeded in a 24-well plate with a coverslip (0.17 mm in thickness) at the bottom of each well for 24 h incubation. Then 5 μg/mL crystal **1** probes were added to the wells and incubated with the PC 12 cells for 12 h in the incubator. The cells were washed three times with 1× phosphate buffered solution (PBS, pH = 7.4) and fixed with 4% paraformaldehyde for about 15 min at room temperature. To examine the effect of MOFs on the organization of microtubular cytoskeleton, the cells on the coverslips were stained by a marker for stable microtubules. The cells were first permeabilized by Triton X-100 (0.5% in PBS) for 2 h at room temperature and blocked by FBS (2% in PBS) and bovine serum albumin (BSA, 2% in PBS) for another 2 h. Then the cells were cultured with Alexa-Fluor 647-conjugated β-tubulin (1:500 in PBS, Cell signaling) at room temperature for 2 h to visualize filamentous tubulin, followed by DAPI (1 μg/mL, Sigma-Aldrich) staining for 5 min to visualize nuclear DNA. Fluorescence imaging of cells was carried out using a confocal laser scanning microscopes with a 60× oil-immersion objective at room temperature in a two-channel mode with the laser excitation wavelengths of 405 nm for DAPI and 633 nm for Alexa-Fluor 647-conjugated β-tubulin, respectively. Both fluorescence and bright-field images of labeled PC12 cells were recorded.

Drug Release. Drug pellets were prepared by compacting ibuprofen-containing porous solids (100 mg) and disintegrating agent sodium carboxymethyl starch (20 mg) with a uniaxial pressure around 2.0 or 4.0 MPa. The release assays were carried out by soaking the samples in a PBS solution (50 mL for each pellet) at 37 °C. Reaction mixture (0.40 mL) was extracted with a syringe after certain periods, and the residual solid was removed by centrifugation and

dx.doi.org/10.1021/jm5004107 | J. Med. Chem. 2014, 57, 5679–5685

passing syringe filter (0.22 μm) to yield a drug containing solution for analysis. The contents of ibuprofen released in PBS solution were determined by high performance liquid chromatography (HPLC) using an Agilent 1200 chromatographic system. Zorbax Eclipse XDB-C18 reverse-phase column (5 μm, 4.6 mm × 250 mm), supplied by Waters, were employed. The mobile phase was composed of 20% (v/v) formic acid and 20% (v/v) nitrile in methanol. The injection volume was 25 μL, the flow rate 0.80 mL/min, and the effluent was monitored at 264 nm. The absorption peak for targeted compounds ibuprofen was observed at about 7.1 min.

■ ASSOCIATED CONTENT

Supporting Information

Ingredients analysis of drug released PBS solution and solid residual. This material is available free of charge via the Internet at http://pubs.acs.org.

■ AUTHOR INFORMATION

Corresponding Author

*Phone: +86-571-87952873. E-mail: yuyang@zju.edu.cn.

Author Contributions

The manuscript was written through contributions of all authors. All authors have given approval to the final version of the manuscript.

Notes

The authors declare no competing financial interest.

■ ACKNOWLEDGMENTS

We gratefully acknowledge the financial support for this work from the National Natural Science Foundation of China (nos. 51229201 and 51372221) and Natural Science Foundation of Zhejiang Province (no. LY12E02004).

■ ABBREVIATIONS USED

PC12, pheochromocytoma 12; MTT, 3-(4,5-dimethylthiazol-2-yl)-2,5-diphenyl tetrazolium; MOFs, metal−organic frameworks; XPS, X-ray photoelectron spectroscopy; SBUs, secondary building units; PCMs, phase-change materials; DMEM, Dulbecco's Modified Eagle's Medium; FBS, fetal bovine serum; DAPI, 4′,6-diamidino-2-phenylindole

■ REFERENCES

(1) (a) Suh, M. P.; Park, H. J.; Prasad, T. K.; Lim, D.-W. Hydrogen storage in metal−organic frameworks. *Chem. Rev.* **2012**, *112*, 782−835. (b) Murray, L. J.; Dinca, M.; Long, J. R. Hydrogen storage in metal−organic frameworks. *Chem. Soc. Rev.* **2009**, *38*, 1294−1314. (c) Wu, H.; Zhou, W.; Yildirim, T. High-capacity methane storage in metal−organic frameworks M2(dhtp): the important role of open metal sites. *J. Am. Chem. Soc.* **2009**, *131*, 4995−5000. (d) Guo, Z.; Wu, H.; Srinivas, G.; Zhou, Y.; Xiang, S.; Chen, Z.; Yang, Y.; Zhou, W.; O'Keeffe, M.; Chen, B. A Metal−organic framework with optimized open metal sites and pore spaces for high methane storage at room temperature. *Angew. Chem., Int. Ed.* **2011**, *50*, 3178−3181. (e) Herm, Z. R.; Wiers, B. M.; Mason, J. A.; van Baten, J. M.; Hudson, M. R.; Zajdel, P.; Brown, C. M.; Masciocchi, N.; Krishna, R.; Long, J. R. Separation of hexane isomers in a metal−organic framework with triangular channels. *Science* **2013**, *340*, 960−964. (f) Farrusseng, D. *Metal-Organic Frameworks: Applications from Catalysis to Gas Storage*. Wiley-VCH: Weinheim, Germany, 2011; pp 1−392.

(2) (a) Seo, J. S.; Whang, D.; Lee, H.; Jun, S. I.; Oh, J.; Jeon, Y. J.; Kim, K. A homochiral metal−organic porous material for enantioselective separation and catalysis. *Nature* **2000**, *404*, 982−986. (b) Ma, L.; Abney, C.; Lin, W. Enantioselective catalysis with homochiral metal−organic frameworks. *Chem. Soc. Rev.* **2009**, *38*, 1248−1256.

(3) Wang, C.; Liu, D.; Lin, W. Metal−organic frameworks as a tunable platform for designing functional molecular materials. *J. Am. Chem. Soc.* **2013**, *135*, 13222−13234.

(4) (a) Li, Y.; Zhang, S.; Song, D. A luminescent metal−organic framework as a turn-on sensor for DMF vapor. *Angew. Chem., Int. Ed.* **2013**, *52*, 710−713. (b) Lan, A.; Li, K.; Wu, H.; Olson, D. H.; Emge, T. J.; Ki, W.; Hong, M.; Li, J. A luminescent microporous metal−organic framework for the fast and reversible detection of high explosives. *Angew. Chem., Int. Ed.* **2009**, *48*, 2334−2338. (c) Takashima, Y.; Martinez, V. M.; Furukawa, S.; Kondo, M.; Shimomura, S.; Uehara, H.; Nakahama, M.; Sugimoto, K.; Kitagawa, S. Molecular decoding using luminescence from an entangled porous framework. *Nature. Commun.* **2011**, *2*, 168.

(5) Horcajada, P.; Chalati, T.; Serre, C.; Gillet, B.; Sebrie, C.; Baati, T.; Eubank, J. F.; Heurtaux, D.; Clayette, P.; Kreuz, C.; Chang, J.-S.; Hwang, Y. K.; Marsaud, V.; Bories, P.-N.; Cynober, L.; Gil, S.; Ferey, G.; Couvreur, P.; Gref, R. Porous metal−organic framework nanoscale carriers as a potential platform for drug delivery and imaging. *Nature Mater.* **2010**, *9*, 172−178.

(6) (a) di Nunzio, M. R.; Agostoni, V.; Cohen, B.; Gref, R.; Douhal, A. A "ship in a bottle" strategy to load a hydrophilic anticancer drug in porous metal organic framework nanoparticles: efficient encapsulation, matrix stabilization, and photodelivery. *J. Med. Chem.* **2014**, *57*, 411−420. (b) Horcajada, P.; Gref, R.; Baati, T.; Allan, P. K.; Maurin, G.; Couvreur, P.; Férey, G.; Morris, R. E.; Serre, C. Metal−organic frameworks in biomedicine. *Chem. Rev.* **2012**, *112*, 1232−1268.

(7) (a) An, J.; Geib, S. J.; Rosi, N. L. Cation-triggered drug release from a porous zinc−adeninate metal−organic framework. *J. Am. Chem. Soc.* **2009**, *131*, 8376−8377. (b) Sun, C.-Y.; Qin, C.; Wang, C.-G.; Su, Z.-M.; Wang, S.; Wang, X.-L.; Yang, G.-S.; Shao, K.-Z.; Lan, Y.-Q.; Wang, E.-B. Chiral nanoporous metal−organic frameworks with high porosity as materials for drug delivery. *Adv. Mater.* **2011**, *23*, 5629−5632.

(8) (a) Taylor-Pashow, K. M. L.; Rocca, J. D.; Xie, Z.; Tran, S.; Lin, W. Postsynthetic modifications of iron−carboxylate nanoscale metal−organic frameworks for imaging and drug delivery. *J. Am. Chem. Soc.* **2009**, *131*, 14261−14263. (b) Burrows, A. D.; Jurcic, M.; Keenan, L. L.; Lane, R. A.; Mahon, M. F.; Warren, M. R.; Nowell, H.; Paradowski, M.; Spencer, J. Incorporation by coordination and release of the iron chelator drug deferiprone from zinc-based metal−organic frameworks. *Chem. Commun.* **2013**, *49*, 11260−11262. (c) Horcajada, P.; Serre, C.; Maurin, G.; Ramsahye, N. A.; Balas, F.; Vallet-Regí, M. a.; Sebban, M.; Taulelle, F.; Férey, G. r. Flexible porous metal−organic frameworks for a controlled drug delivery. *J. Am. Chem. Soc.* **2008**, *130*, 6774−6780.

(9) Millward, A. R.; Yaghi, O. M. Metal−organic frameworks with exceptionally high capacity for storage of carbon dioxide at room temperature. *J. Am. Chem. Soc.* **2005**, *127*, 17998−17999.

(10) Dietzel, P. D. C.; Johnsen, R. E.; Blom, R.; Fjellvåg, H. Structural changes and coordinatively unsaturated metal atoms on dehydration of honeycomb analogous microporous metal−organic frameworks. *Chem.—Eur. J.* **2008**, *14*, 2389−2397.

(11) McKinlay, A. C.; Xiao, B.; Wragg, D. S.; Wheatley, P. S.; Megson, I. L.; Morris, R. E. Exceptional behavior over the whole adsorption−storage−delivery cycle for NO in porous metal organic frameworks. *J. Am. Chem. Soc.* **2008**, *130*, 10440−10444.

(12) Bloch, E. D.; Murray, L. J.; Queen, W. L.; Chavan, S.; Maximoff, S. N.; Bigi, J. P.; Krishna, R.; Peterson, V. K.; Grandjean, F.; Long, G. J.; Smit, B.; Bordiga, S.; Brown, C. M.; Long, J. R. Selective binding of O_2 over N_2 in a redox−active metal−organic framework with open iron(II) coordination sites. *J. Am. Chem. Soc.* **2011**, *133*, 14814−14822.

(13) Bernini, M. C.; Fairen-Jimenez, D.; Pasinetti, M.; Ramirez-Pastor, A. J.; Snurr, R. Q. Screening of biocompatible metal−organic frameworks as potential drug carriers using Monte Carlo simulations. *J. Mater. Chem., B* **2014**, *2*, 766−774.

(14) Aronniemi, M.; Lahtinen, J.; Hautojärvi, P. Characterization of iron oxide thin films. *Surf. Interface Anal.* **2004**, *36*, 1004−1006.

(15) Horcajada, P.; Serre, C.; Vallet-Regí, M.; Sebban, M.; Taulelle, F.; Férey, G. Metal−organic frameworks as efficient materials for drug delivery. *Angew. Chem., Int. Ed.* **2006**, *45*, 5974−5978.

(16) Piga, R.; Saito, Y.; Yoshida, Y.; Niki, E. Cytotoxic effects of various stressors on PC12 cells: involvement of oxidative stress and effect of antioxidants. *Neurotoxicology* **2007**, *28*, 67−75.
(17) Zhang, Y.; Ali, S. F.; Dervishi, E.; Xu, Y.; Li, Z.; Casciano, D.; Biris, A. S. Cytotoxicity effects of graphene and single-wall carbon nanotubes in neural phaeochromocytoma-derived PC12 cells. *ACS Nano* **2010**, *4*, 3181−3186.
(18) Masters, J. R. W. *Animal Cell Culture: A Practical Approach*, 3rd ed.; Oxford University Press: Oxford, 2000; pp 190 and 207.
(19) Jeong, B.; Bae, Y. H.; Kim, S. W. Drug release from biodegradable injectable thermosensitive hydrogel of PEG−PLGA−PEG triblock copolymers. *J. Controlled Release* **2000**, *63*, 155−163.
(20) Choi, S.-W.; Zhang, Y.; Xia, Y. A temperature-sensitive drug release system based on phase-change materials. *Angew. Chem., Int. Ed.* **2010**, *49*, 7904−7908.